processes

MDPI

Article

Assessing the Impact of Ethanol/Biodiesel/Diesel Blends and Nanoparticle Fuel Additives on Performance and Emissions in a DI Diesel Engine with EGR Integration: An Experimental Study

Raouf Mobasheri [1,*], Abdel Aitouche [1,2], Sadegh Pourtaghi Yousefdeh [3] and Abbas Zarenezhad Ashkezari [3]

[1] Junia, Smart Systems and Energies, F-59000 Lille, France
[2] Univ. Lille, CNRS, Centrale Lille, UMR 9189—CRIStAL—Centre de Recherche en Informatique Signal et Automatique de Lille, F-59000 Lille, France
[3] Department of Mechanical Engineering, Imam Khomeini Marine Sciences University, Nowshahr 4651783311, Iran
* Correspondence: raouf.mobasheri@junia.com

Abstract: In this paper, the effect of nano-particles along with EGR rates was experimentally assessed on the performance and emission of a DI diesel engine fueled by biodiesel and ethanol. For this purpose, three levels of TiO_2 nanoparticles (0, 40, and 60 ppm) were added to biodiesel/diesel blends in the proportions of 0, 10, and 20% biodiesel with ethanol at levels of 0, 4, and 6%. EGR rates were used at 0, 20, and 30%. A total of 31 fuel samples with different ethanol, biodiesel, TiO_2 nano-additives, and EGR rates were tested at different speeds. The equation for this combination is B_xE_y + EGR_w + TiO_{2z}, where x, y, w, and z are the percentages of biodiesel, ethanol, EGR, and TiO_2. The results showed that the mixture of B10E4 + EGR20 + $TiO_2$60, reduced the amount of NO_x, CO, and HC by 10, 12.4, and 17%. Moreover, due to the significant reduction of emissions and performance improvement, the combinatory method of EGR–TiO_2 nano-additives can be used as an effective formula for diesel engines fueled with ethanol/biodiesel/diesel blends.

Keywords: biodiesel; ethanol; TiO_2 nano additive; EGR; emission

Citation: Mobasheri, R.; Aitouche, A.; Pourtaghi Yousefdeh, S.; Zarenezhad Ashkezari, A. Assessing the Impact of Ethanol/Biodiesel/Diesel Blends and Nanoparticle Fuel Additives on Performance and Emissions in a DI Diesel Engine with EGR Integration: An Experimental Study. *Processes* **2023**, *11*, 1266. https://doi.org/10.3390/pr11041266

Academic Editor: Jiaqiang E

Received: 21 February 2023
Revised: 28 March 2023
Accepted: 17 April 2023
Published: 19 April 2023

1. Introduction

Many researchers have recently become interested in the use of oxygenated fuels such as biodiesel and ethanol in diesel engines due to the implementation of severe limits on pollutant emissions [1–3]. Biodiesel, which is a high chain fatty acid monoalkyl ester, is obtained from renewable sources such as vegetable oils, waste, and animal fats [4]. Biodiesel, depending on the type of oil used in its production, contains 10 to 12 percent of oxygen approximately [5,6]. Ethanol as a renewable fuel can be produced by fermenting plant products that contain large amounts of sugar. Additionally, any compound that can be converted to sugar, such as starch and cellulose, is used in the production of ethanol [7]. Ethanol contains about 35% of oxygen, which helps to reduce soot and PM [8,9]. According to the studies, the mixtures of biodiesel and ethanol up to 20 vol% can be combined with pure diesel without any significant engine hardware modification [10–12]. In 2014, Karthikeyan et al. [13] investigated the performance, combustion, and emission characteristics of a single-cylinder engine for various mixtures of biodiesel and zinc oxide nanocatalysts. They also evaluated the properties of the prepared fuels, such as flash point, viscosity, cetane number, and calorific value. Their results showed that the addition of zinc oxide nanocatalysts accelerated the reaction rate and increased NO_x. In an experimental study conducted by Saravana in 2015 [14], the emissions and performance of a diesel engine fueled by pentanol were examined. Their results indicated that all prepared mixtures from pentanol had higher HC and CO emissions than pure diesel fuel. In 2017, Yilmaz et al. [15] experimentally evaluated the use of diesel, biodiesel, and pentanol fuels in a four-stroke single-cylinder

diesel engine under different engine loads. The results showed that the use of biodiesel and pentanol increased NO_x and BSFC. In 2019, Devarajan et al. [16] investigated the combustion and emission characteristics of a single-cylinder diesel engine by adding the silver oxide nanoparticles at different particle sizes to biodiesel. The results showed that the use of biodiesel increases the amount of NO_x and the addition of nanoparticles reduces it. In 2020, Uyumaz [17] examined the combustion, performance, and emission characteristics of a diesel engine using linseed oil biodiesel. They concluded that with increasing the percentage of biodiesel, the amounts of NO_x, CO_2 emissions, as well as thermal efficiency, decreased. Disadvantages of oxygenated fuels include reducing power and torque and increasing fuel consumption, which has been reported in many references [18,19]. The nanoparticles can improve power and torque as well as reduce fuel consumption [20,21]. However, the addition of TiO_2 nanoparticles accelerates the reaction rate and increases NO_x emissions [22,23]. On the other hand, the EGR system is one of the methods that can be used to reduce NO_x emissions [24,25]. For this purpose, laboratory tests were applied to investigate the effect of TiO_2 nano-additive along with EGR rates on performance and emissions of a DI diesel engine fueled with ethanol and biodiesel.

2. Materials and Methods

2.1. Fuel

The high purity ethanol, pure diesel, and biodiesel were applied in this research. Table 1 shows the properties of the fuels. Biodiesel was mixed with pure diesel (D100) at 10 and 20 vol% and named B10E0 and B20E0. Ethanol was mixed with pure diesel at two levels (4 vol% and 6 vol%) and was shown as B0E4 and B0E6. A mixture was also prepared by a simultaneous combination of biodiesel–ethanol and was named B10E4. Previous studies on the mixing of ethanol and diesel [19,26,27] showed that the phase separation in the ethanol–diesel mixture does not occur at temperatures above 10 °C. It should be noted that, in the present work, all operating conditions are at temperatures above 20 °C.

Table 1. Properties of diesel, biodiesel, and ethanol.

Fuel Property	Units	Diesel	Biodiesel	Ethanol	Method
Oxygen content	wt.%	0	11	35	D5293
Carbon content	wt.%	87	78	51	D5291
Hydrogen content	wt.%	13	11	14	D5292
Cetane number	-	55	62	7	D6890
Calorific value	MJ kg^{-1}	43.37	34.35	27.52	D240
Flash point	°C	69.8	110.15	13	D93
Kinematic viscosity @ 40 °C	mm^2 s^{-1}	3.42	4.19	1.13	D445
Density @ 15 °C	kg m^{-3}	847.7	887.3	794.9	D127

2.2. Preparation of Fuel Blends with TiO_2 Additive

Bandalin Sonopuls HD 3400 ultrasonic homogenizer has been used to add TiO_2 nanoparticles and prepare a homogeneous mixture. This process was performed for 30 min to provide the uniform distribution of nanoparticles and stability of the prepared mixtures. The average size of the nanoparticles is smaller than the diameter of the injector nozzle, so there will be no disturbance in the fuel flow path. TiO_2 nanoparticles were added to diesel–ethanol–biodiesel mixtures at 40 and 60 ppm levels. The main characteristics of TiO_2 are given in Table 2.

2.3. Exhaust Gas Recirculation (EGR)

Recirculating some of the exhaust gases to the inlet manifold and combining it with fresh air is an effective way to reduce NO_x emissions. Numerous studies on the EGR system have shown that NO_x reduction cannot be achieved without cooling the exhaust gases. The high exhaust gas temperatures can increase NO_x formation [28]. For this purpose, an

external cooled EGR system was used at two rates of 10 and 20%. This system reduces the maximum temperature and oxygen concentration and increases the specific heat of the mixture inside the combustion chamber. The EGR rate is controlled by the EGR valve and an orifice meter is used to measure the flow rate of the exhaust gas. Using Equation (1), the EGR value is expressed as a percentage [29]:

$$\%EGR = \left(\frac{CO_2 \text{ intake}}{CO_2 \text{ exhaust}} \right) \times 100 \quad (1)$$

Table 2. Properties of TiO_2.

Chemical Name	Titanium Dioxide
Purity	>99%
Form	Powder
Color	White
Average particle size	20 nm
Molecular weight	82.3 g/mol
Chemical abstract service (CAS) number	12188-41-9

2.4. Experimental Setup

A four-stroke six-cylinder diesel engine with the power of 62 kW was applied to investigate the combined effect of TiO_2 nano-additives and EGR rates on combustion and emission characteristics of biodiesel–ethanol–diesel blends. The engine specifications are given in Table 3 as well as the schematic of the testbed in Figure 1. To measure torque and power, a 400 kW hydraulic dynamometer with an accuracy of ±2 Nm is used, which creates a brake force against the rotation of the motor by creating a magnetic field. Eddy current dynamometer is equipped with a data collection system that is cooled by water. While no load is applied to the motor, the dynamometer rotates freely on the bearings. The SWPF-60A mass flowmeter with an accuracy of 0.01 kg/hr was used to measure fuel consumption. Temperature sensors are of the resistance thermometer (R) type, which can measure temperatures up to 1900 degrees. Their accuracy is ±1 degree and their coil is made of platinum with a base resistance of 100 Ω. A magnetic tachometer attached to the output shaft was used to measure the engine speed. Testo 350 was also used to measure the amounts of NO_x, CO, CO_2, and HC in all of the engine testing. It should be noted that the emissions analyzer is carefully calibrated before the tests to ensure the accuracy of the measurements. The variations range and calibration of this device are given in Table 4. The test result was analyzed and received in a computer system.

Table 3. Specifications of the test engine.

Manufacturer and Model	LOVOL 1006TG1A
Engine type	Six-cylinder, four-stroke, direct injection, turbocharged
Number of cylinders	6
Cylinder volume	5.99 lit
Bore and stroke	100 * 127 (mm)
Compression ratio	17.5:1
Maximum torque	337 Nm@1400 rpm
Maximum power	62 kW@2000 rpm
Number of holes in the nozzle	5

The range for engine speed was 1000 to 1800 rpm. First, the engine warms up for about 10 min to reach a steady state in terms of inlet and outlet water temperature and oil temperature, and the tests were performed in an almost stable state. To prepare the engine setup, the oil level inside the oil pan is checked to be full. The water flow is then opened to the dynamometer and the needle valve is opened with the maximum water flow obtained, ensuring that the dynamometer seals are lubricated. The water flow is reduced

to the point of dripping and the engine is started. The engine is allowed to run for about 10 min to warm up. The throttle control lever is then advanced to its maximum position and the maximum speed of the engine is recorded.

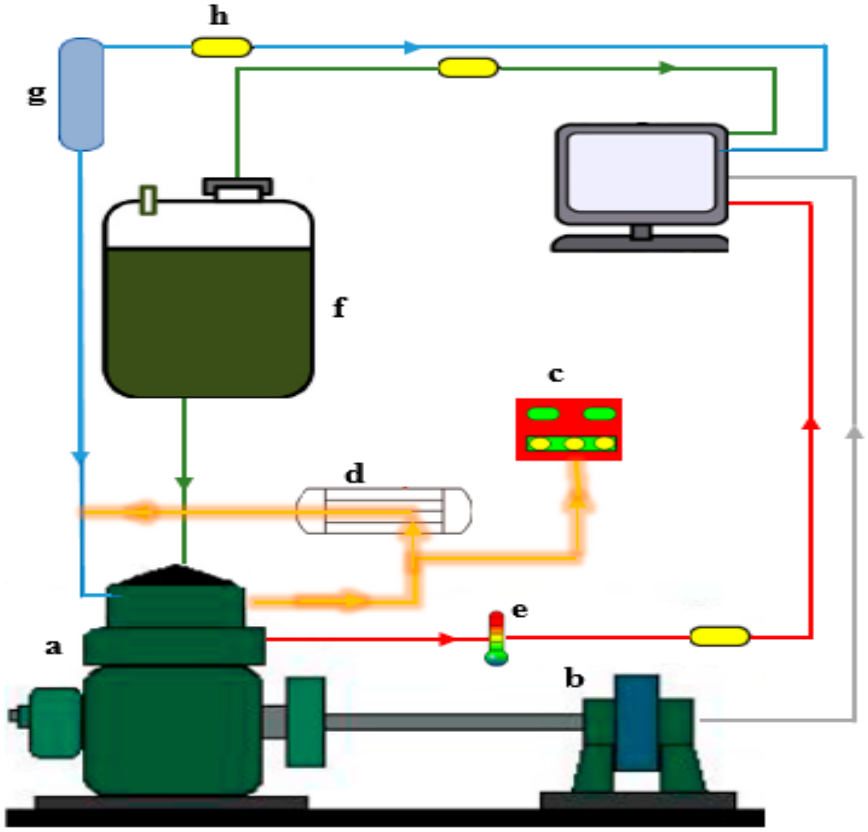

Figure 1. Schematic arrangement of the engine test bed: (**a**) diesel engine, (**b**) dynamometer, (**c**) gas analyzer, (**d**) EGR system, (**e**) thermometer, (**f**) fuel tank, (**g**) air tank, (**h**) transducer.

Table 4. Specification of the Testo 350 emission analyzer.

Resolution	Range	Parameter
1 ppm	0–3000 ppm	NO_x
1 ppm	0–5000 ppm	CO
0.1 vol%	0–50 vol%	CO_2
1 ppm	0–40,000 ppm	HC

When the engine reached to the steady state conditions, the amounts of torque, inlet air temperature, fuel mass, amounts of NO_x, CO, CO_2, HC, and BSFC, and exhaust gas temperature and engine speed are recorded. This process was repeated for different operating conditions. After the test, the needle valve was closed. Allow the engine to run for a few minutes in this mode. The engine now turns off and closes the main water valve. It should be noted that the measurements were repeated three times for each sample and their mean value was recorded as the final data. All equipment is calibrated before the tests to avoid possible errors in the laboratory data.

2.5. Uncertainty Analysis

In experimental studies, the calculation of uncertainty is necessary. Uncertainty provides information about the quality of the measured parameters. Regardless of the accuracy of the test, there may be errors in the collection of experimental data for a variety of reasons. To identify these errors, statistical analysis of laboratory data, uncertainty has been used. Fixed and random errors may cause uncertainty in an experimental measurement.

Fixed errors are usually eliminated by calibrating the measuring instruments, but random errors are detected through statistical analysis. In the present work, the uncertainty of the data is calculated from Equation (2):

$$\sigma_m = \frac{\sigma}{n^{0.5}} \quad (2)$$

in which, σ_m is the standard deviation of the mean value, σ is the standard deviation of the set of measurements, and n is the number of measurements at each point (n = 3, for all laboratory results). The uncertainty of the laboratory data is also calculated from Equation (3):

$$X = \frac{\sigma_m}{\bar{x}} \times 100 \quad (3)$$

that X is the uncertainty of the laboratory data. Additionally, the parameter X is calculated with the arithmetic mean of the data. Each test was repeated three times to avoid errors in the recording of laboratory data as much as possible. At each stage, a slight difference may be observed, which is characteristic of experimental work. Irrelevant data are removed to ensure the accuracy of the results and the percentage of uncertainty is obtained by using the obtained relations. For example, as the results show, the recorded data are acceptable for NO_x emissions with ±4%. In other words, in the results of NO_x = 100 ppm, this value will be in the range (96–104), i.e., 100 ± 4 ppm.

3. Discussion on Results

3.1. Brake Power

Figures 2 and 3 show the power variation at different speeds for diesel–ethanol–biodiesel blends using TiO_2 nano-additive and EGR system.

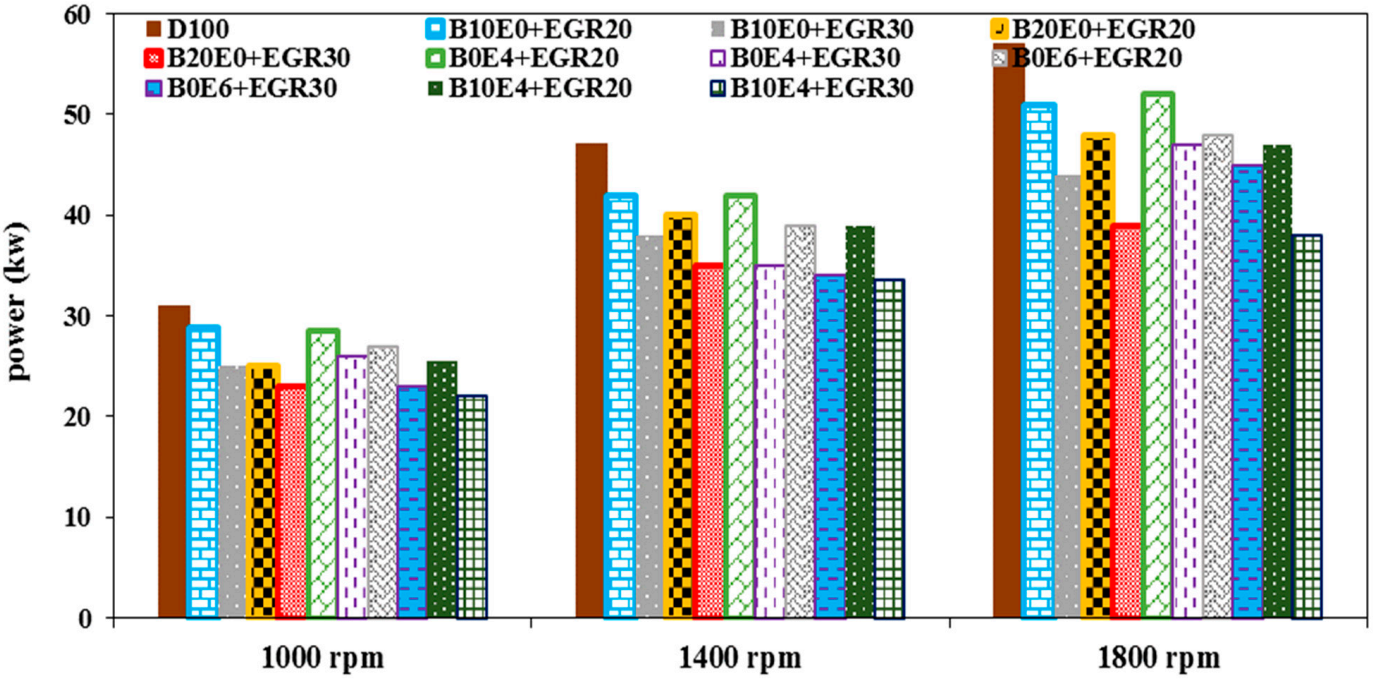

Figure 2. Variation of power for diesel/ethanol/biodiesel blends at EGR = 20, 30%, and various engine speeds.

Figure 2 shows the effect of EGR rates (20% and 30%) on the power for prepared fuel blends. It is observed that, with increasing the percentage of EGR, the output power decreases. The amount of output power when using B10E4 + EGR30 at the different speeds is between 13.8 to 19.2% less than when using B10E4 + EGR20. The minimum power was observed in B20E0 + EGR30, which reduced the power by an average of 27.8% at different

speeds. B0E6 + EGR30 also reduced the output power compared to D100 at speeds of 1000, 1400, and 1800 rpm by 26, 27.7, and 21.1%. Reducing the amount of oxygen in the combustion chamber can be the main reason for reducing the power by using the EGR system [30–32].

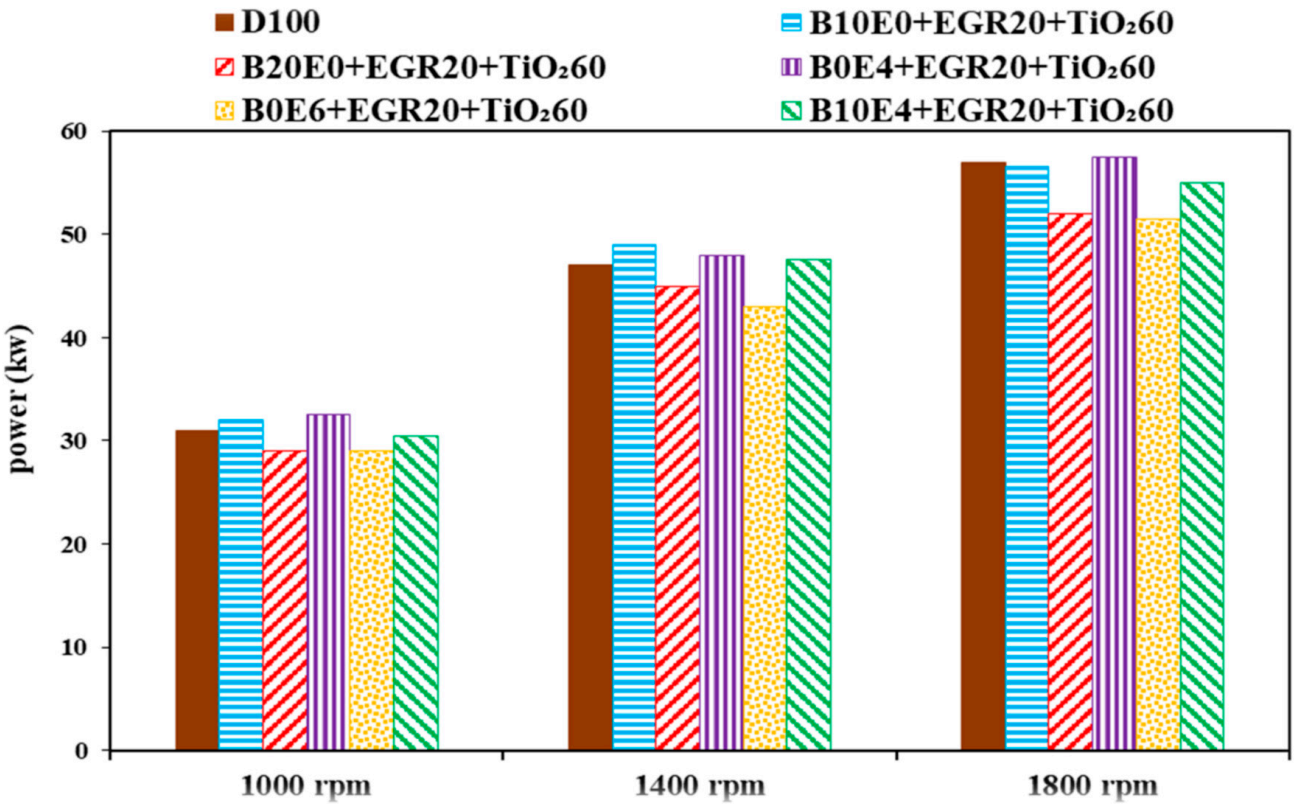

Figure 3. Variation of power for diesel/ethanol/biodiesel blends at EGR = 20%, TiO_2 = 60 ppm, and various engine speeds.

The effect of simultaneous EGR = 20% and TiO_2 = 60 ppm on the output power of the diesel–ethanol–biodiesel blends is shown in Figure 3. It can be seen that the B0E4 + EGR20 + $TiO_2$60 mixture increased the output power by an average of 2.5% compared to the D100 at different speeds.

3.2. Torque

Torque variations at different speeds for prepared mixtures with TiO_2 nanoparticles and the EGR system are shown in Figures 4 and 5. Variations of engine torque for diesel-ethanol–biodiesel blends due to the addition of TiO_2 nanoparticles at 40 and 60 ppm at different speeds are shown in Figure 4. It is observed that by increasing the percentage of nanoparticles, the brake torque increases. The B0E4 + $TiO_2$60 and B10E0 + $TiO_2$60 increased the torque by an average of 2.8 to 3% compared to D100 at different speeds. Using the B10E4 + $TiO_2$60 blend, increased the amount of torque compared to the B10E4 + $TiO_2$40 blend, by an average of 4.3% at the different speeds. The higher energy content and the surface-to-volume ratio of TiO_2 can be the main reasons for increasing the torque [33,34].

The effect of simultaneous EGR = 20% and TiO_2 = 60 ppm on the engine torque for diesel–ethanol–biodiesel blends is shown in Figure 5. The B10E4 + EGR20 + $TiO_2$60 at 1000, 1400, and 1800 rpm reduced torque by 3, 7.7, and 6.2% compared to D100.

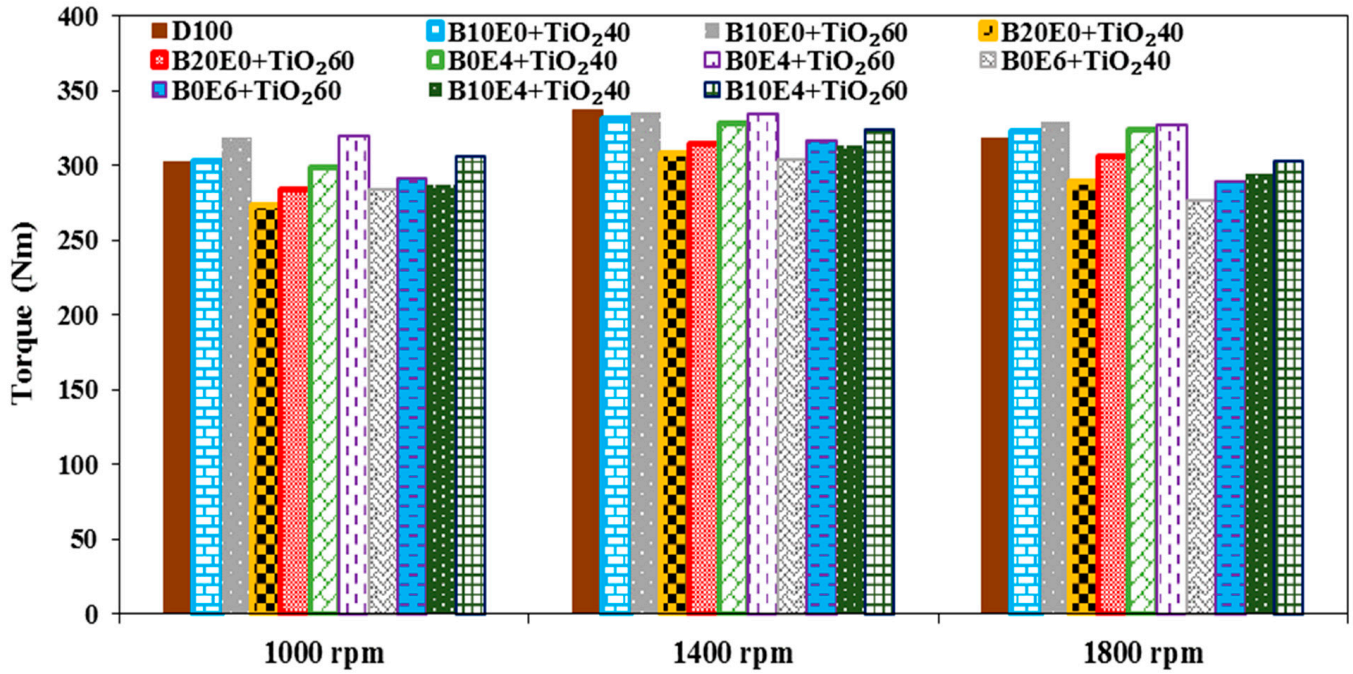

Figure 4. Variation of torque for diesel/ethanol/biodiesel blends at TiO_2 = 40, 60 ppm, and various engine speeds.

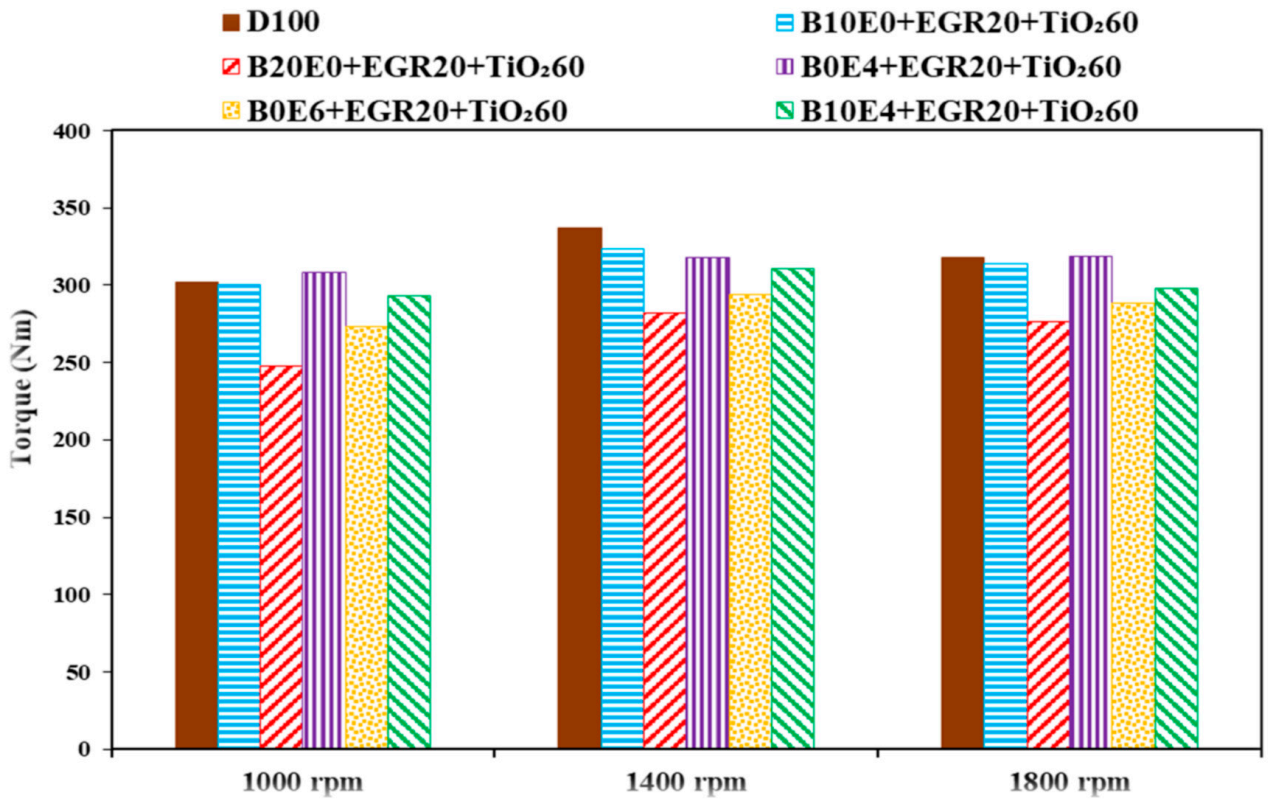

Figure 5. Variation of torque for diesel/ethanol/biodiesel blends at TiO_2 = 40 ppm, EGR = 20%, and various engine speeds.

3.3. BSFC

The fuel consumption characteristics of an engine are generally expressed in terms of fuel consumption in kg of fuel per kW-hr. It is an important parameter that reflects how good engine performance is. It is inversely proportional to the thermal efficiency of the

engine. Brake-specific fuel consumption (BSFC) is the specific fuel consumption on the basis of the brake power (P_b). In other words, BSFC is the measurement of efficiency of fuel by the engine that combusts the fuel–air mixture and produces the rotational motion of the crankshaft. This is used for comparing the efficiency of the engine. BSFC is the ratio of the rate of fuel consumption and the effective power produced from the engine. Mathematically it is expressed as:

$$\text{BSFC} = \frac{\text{Fuel mass flow rate } (\dot{m}_f)}{\text{Brake power } (P_b)} \quad (4)$$

Variations in BSFC at different speeds for prepared fuel blends using TiO_2 nanoparticles and EGR are shown in Figures 6 and 7. The effect of adding TiO_2 nanoparticles at 40 and 60 ppm on the BSFC of diesel–ethanol–biodiesel blends at different speeds is shown in Figure 6. It is observed that with increasing the percentage of nanoparticles, the BSFC decreases. The B10E0 + $TiO_2$60 and B0E4 + $TiO_2$60 decreased BSFC by an average of 11.7% and 12%, at different speeds compared to diesel. Also, the B10E4 + $TiO_2$60 blend reduced the BSFC by 13.5, 13.2, and 16.5%, compared to the B10E4, at 1000, 1400, and 1800 rpm. Improving the combustion process as a result of TiO_2 addition can be the main reason for BSFC reduction [35,36].

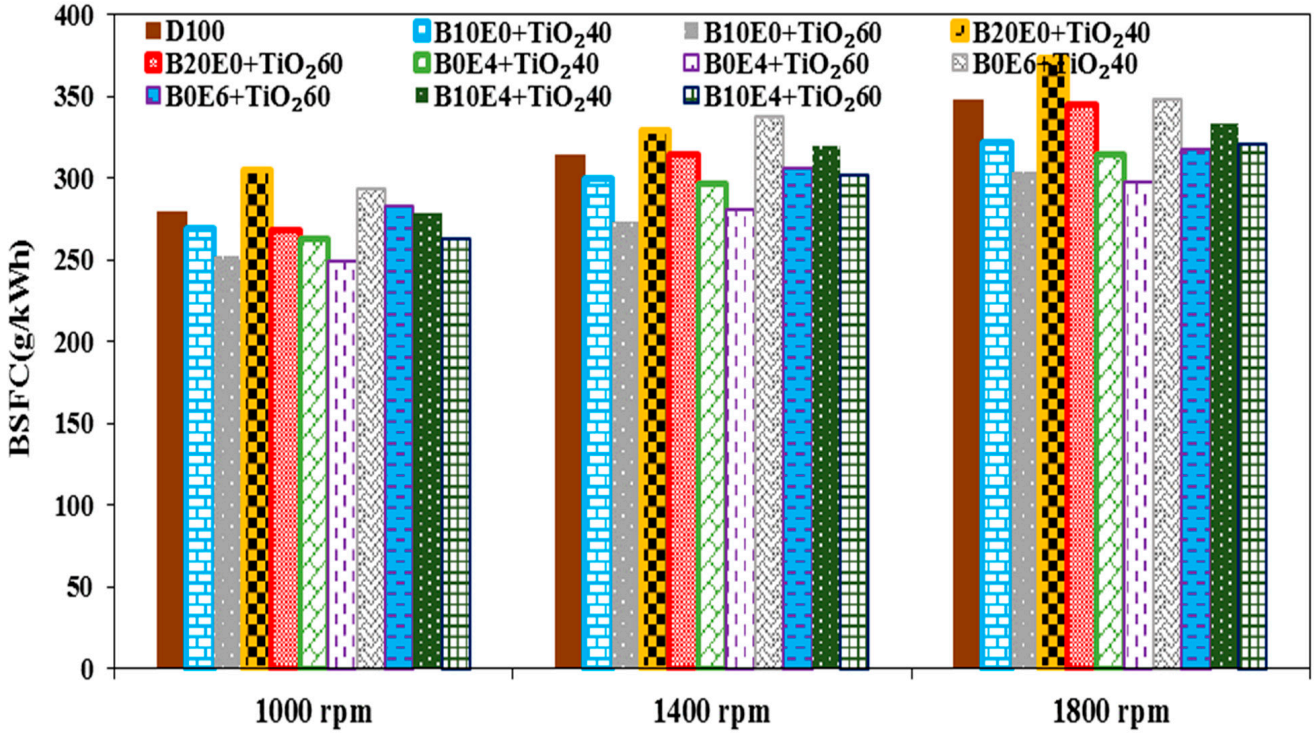

Figure 6. Variation of BSFC for diesel/ethanol/biodiesel blends at TiO_2 = 40, 60 ppm, and various engine speeds.

The effect of simultaneous use of EGR = 20% and TiO_2 = 60 ppm on BSFC for different blends is shown in Figure 7. B10E4 + EGR20 + $TiO_2$60 at 1000, 1400, and 1800 rpm increased BSFC by 4.7, 2.5, and 2% compared to pure diesel.

3.4. Exhaust Gas Temperature

Figures 8 and 9 show the variations of the exhaust gas temperature for the prepared mixtures using the EGR system and TiO_2 nanoparticles. Figure 8 shows that as the percentage of EGR in diesel–ethanol–biodiesel fuels increases, the exhaust gas temperature decreases. The lower oxygen content of the inlet air and the decreasing of the peak combustion temperature can be the reasons for decreasing of the exhaust gas temperature [37].

The minimum exhaust gas temperature was observed for B0E4 + EGR30, which reduced the exhaust temperature by 15, 21, and 13% at 1000, 1400, and 1800 rpm. In addition, the B10E4 + EGR30 blend, reduced the exhaust gas temperature by 15.8% in the different speeds compared to the B10E4 blend.

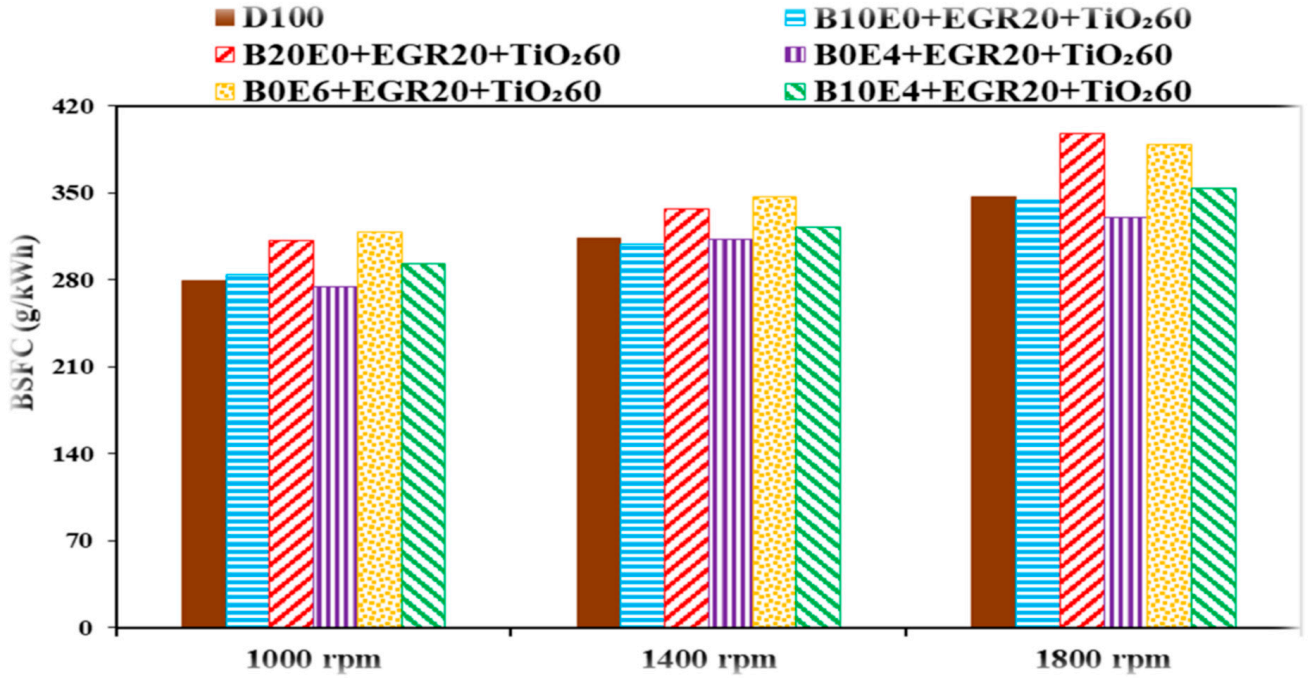

Figure 7. Variation of BSFC for diesel/ethanol/biodiesel blends at EGR = 20%, TiO_2 = 60 ppm, and various engine speeds.

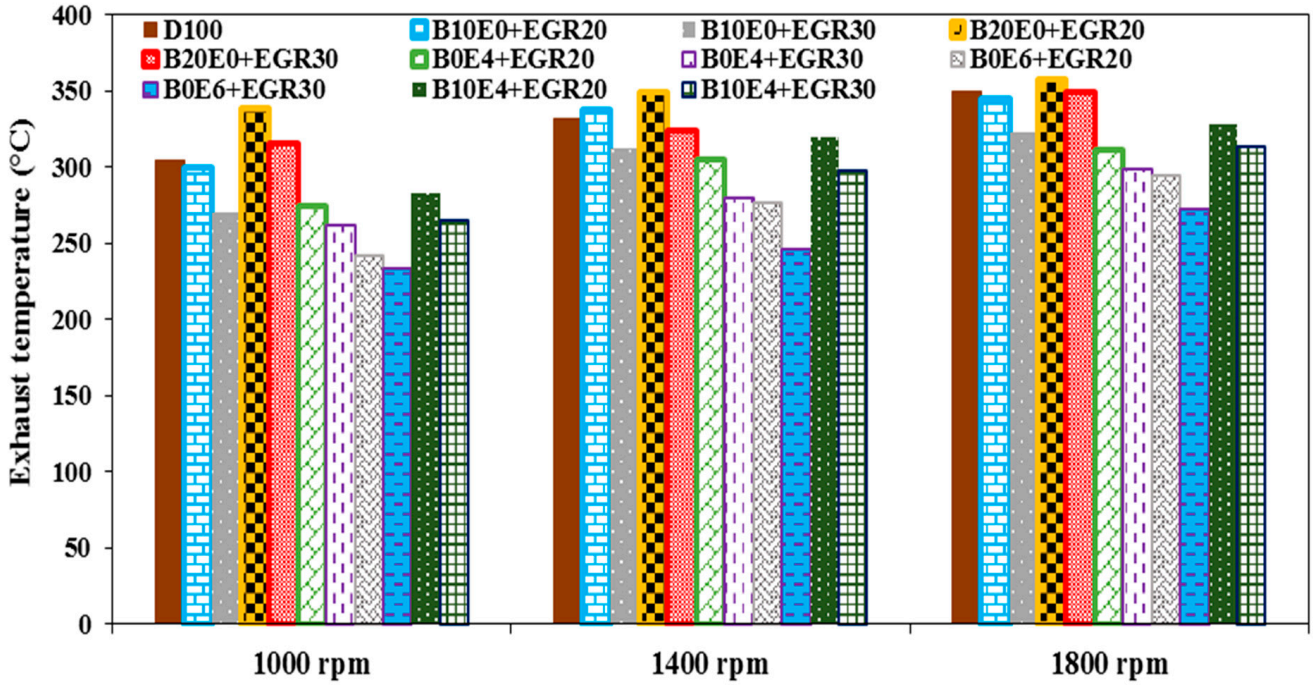

Figure 8. Variation of exhaust temperature for diesel/ethanol/biodiesel blends at EGR = 20, 30%, and various engine speeds.

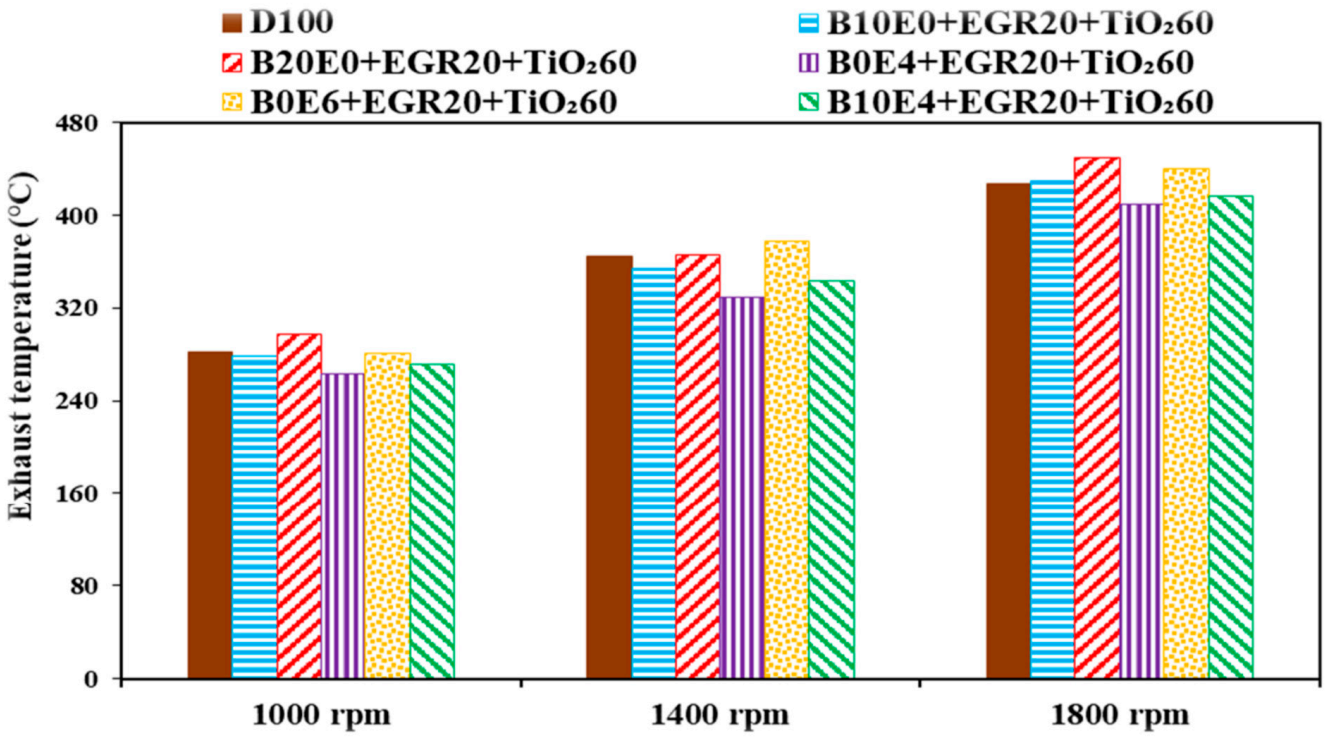

Figure 9. Variation of exhaust temperature for diesel/ethanol/biodiesel blends at EGR = 20%, TiO_2 = 60 ppm, and various engine speeds.

The effect of simultaneous use of EGR = 20% and TiO_2 = 60 ppm on exhaust temperature for different blends is shown in Figure 9. The maximum temperature was observed for B20E0 + EGR20 + $TiO_2$60 with a 3.6% increasing in temperature compared to D100. The minimum temperature was recorded for B0E4 + EGR20 + $TiO_2$60, which showed an average reduction of 7% in the exhaust gas temperature compared to D100 at different speeds.

3.5. NO_x

Variations of NO_x at different speeds for prepared blends are shown in Figures 10 and 11. As can be seen, NO_x emission decreases with increasing speed. Figure 10 shows that with increasing the percentage of TiO_2 in the mixture, the amount of NO_x increases. The maximum amount of NO_x was recorded for B20E0 + $TiO_2$60, which increased the NO_x by 27.5, 26.7, and 35.8% at 1000, 1400, and 1800 rpm. Also, the B10E4 + $TiO_2$60 blend, increased NO_x emission by 2.9% compared to the B10E4 + $TiO_2$40 at different speeds. With increasing of the percentage of TiO_2 in the mixture, more oxygen atoms are available to react with nitrogen atoms in the combustion chamber, increasing the combustion temperature, which can be the main reason for increasing of NO_x emission [38–40].

The effect of EGR = 20% and TiO_2 = 60 ppm on NO_x emission for different blends is shown in Figure 11. The B20E0 + EGR20 + $TiO_2$60 increased NO_x by an average of 6.2% compared to D100 at different speeds. Additionally, the minimum amount of NO_x was recorded for B0E4 + EGR20 + $TiO_2$60 with a 13% reduction compared to D100.

3.6. CO Emission

Figures 12 and 13 show the variations of CO emission for the different mixtures with EGR system and TiO_2 nanoparticles. As can be seen the B10E0 + EGR30 blend increases the amount of CO by 6.7% compared to the B10E0 + E,GR20, at the different speeds. The B10E4 + EGR30 blend also increased CO emission by an average of 4.8% compared to B10E4 + EGR20.

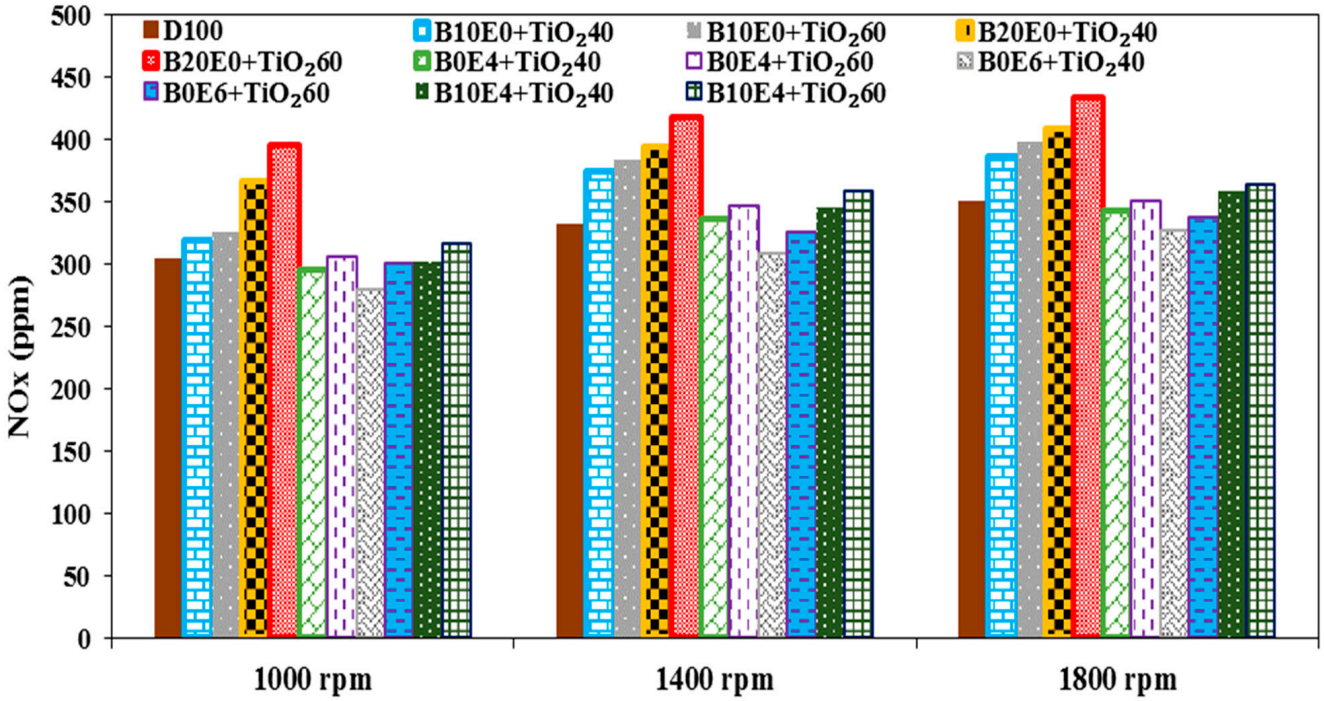

Figure 10. Variation of NO_x for diesel/ethanol/biodiesel blends at TiO_2 = 40, 60 ppm, and various engine speeds.

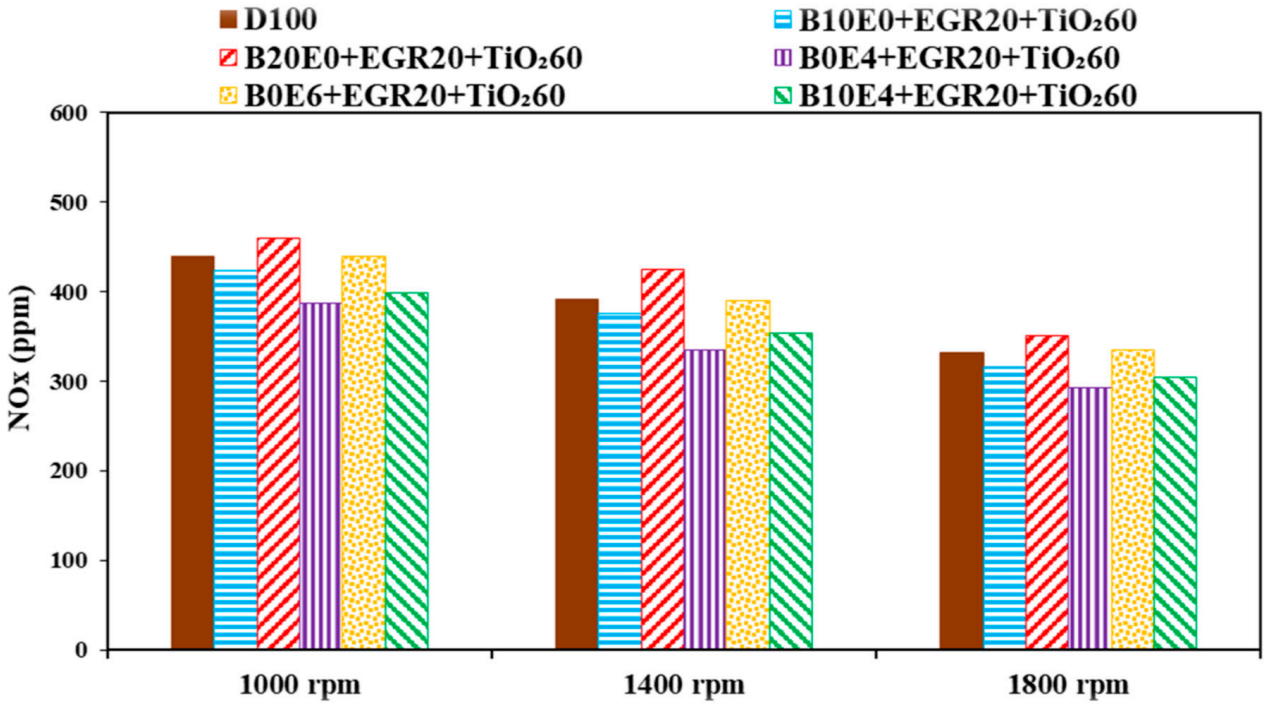

Figure 11. Variation of NO_x for diesel/ethanol/biodiesel blends at EGR = 20%, TiO_2 = 60 ppm, and various engine speeds.

The effect of EGR and TiO_2 in the prepared mixtures on the amount of CO is shown in Figure 13. It is observed that the B10E4 + EGR20 + $TiO_2$60 at 1000, 1400, and 1800 rpm reduces CO by 5.9, 10, and 12.5% compared to D100.

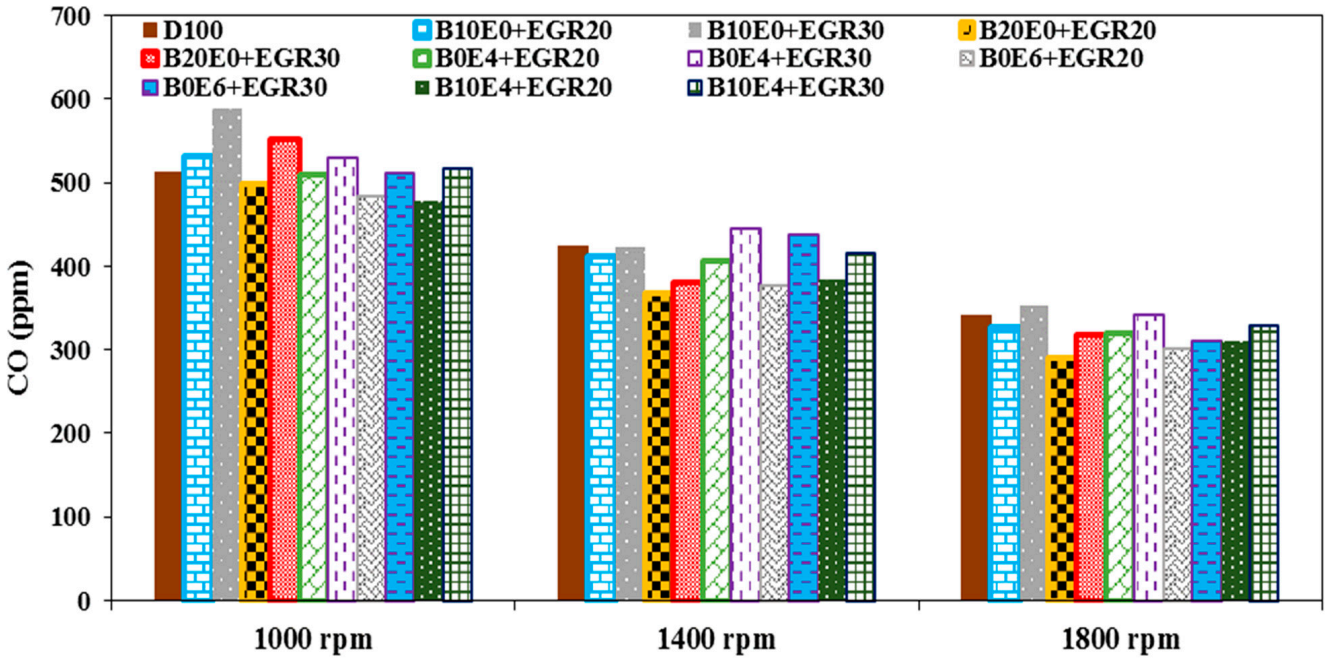

Figure 12. Variation of CO for diesel/ethanol/biodiesel blends at EGR = 20, 30%, and various engine speeds.

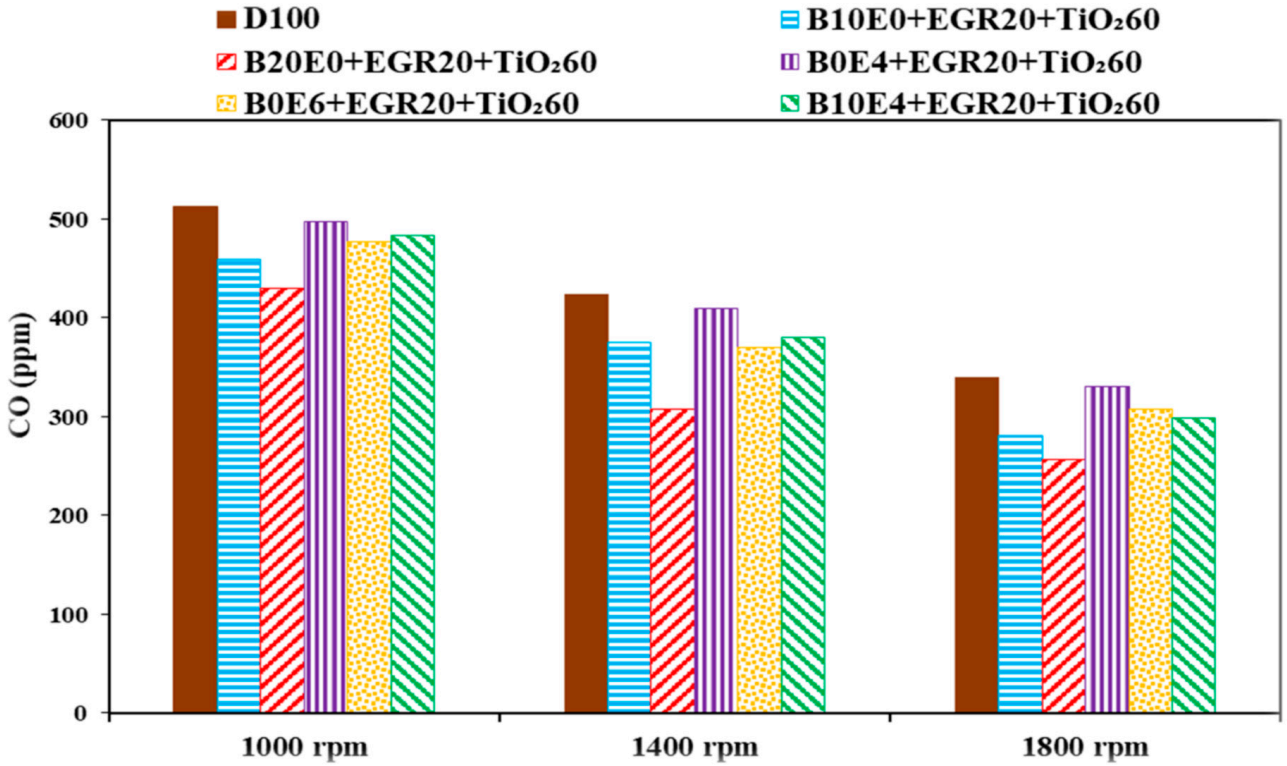

Figure 13. Variation of CO for diesel/ethanol/biodiesel blends at EGR = 20%, TiO_2 = 60 ppm, and various engine speeds.

3.7. CO_2 Emission

Variations of CO_2 emission for diesel–ethanol–biodiesel mixtures by using TiO_2 and EGR are shown in Figures 14 and 15. The effect of adding TiO_2 nanoparticles at 40 and 60 ppm on the CO_2 emission of different blends is shown in Figure 14. It is observed that with increasing of TiO_2 in the blends, the amount of CO_2 increases. Improving the

combustion process can be the main reason for the increase in CO_2 [41]. In addition, the B20E0 + $TiO_2$60 at 1000, 1400, and 1800 rpm increased CO_2 by 17.1, 28, and 11.4% compared to D100.

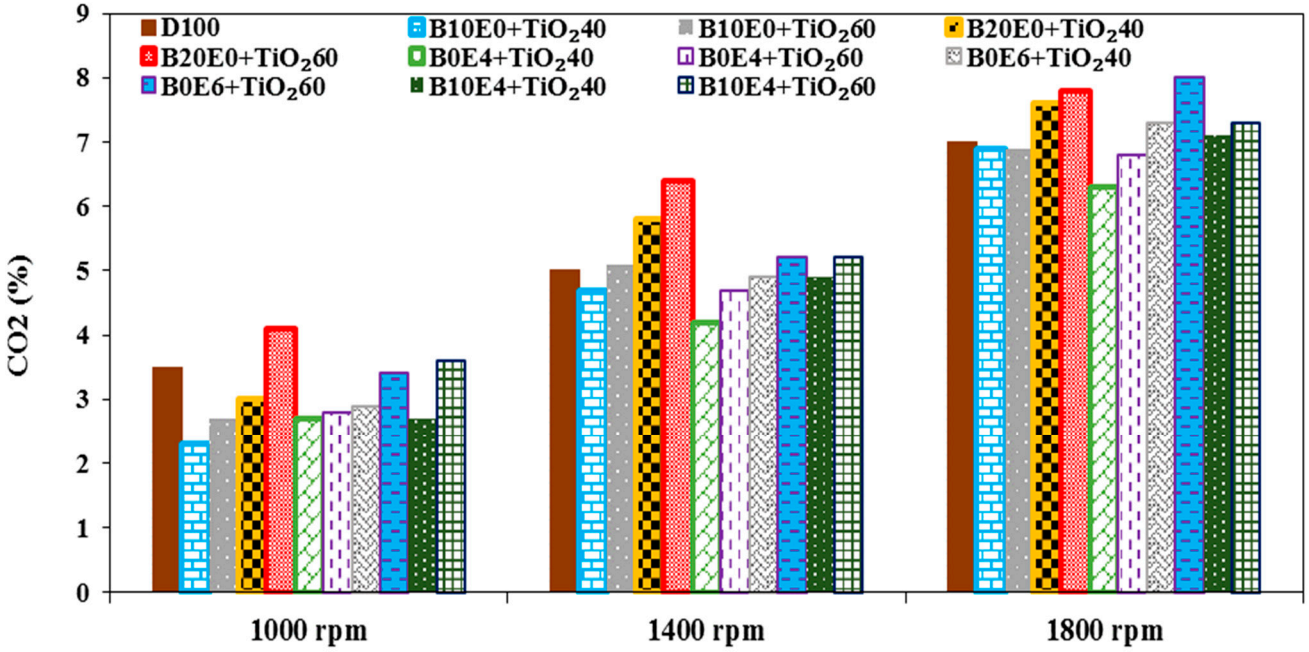

Figure 14. Variation of CO_2 for diesel/ethanol/biodiesel blends at TiO_2 = 40, 60 ppm, and various engine speeds.

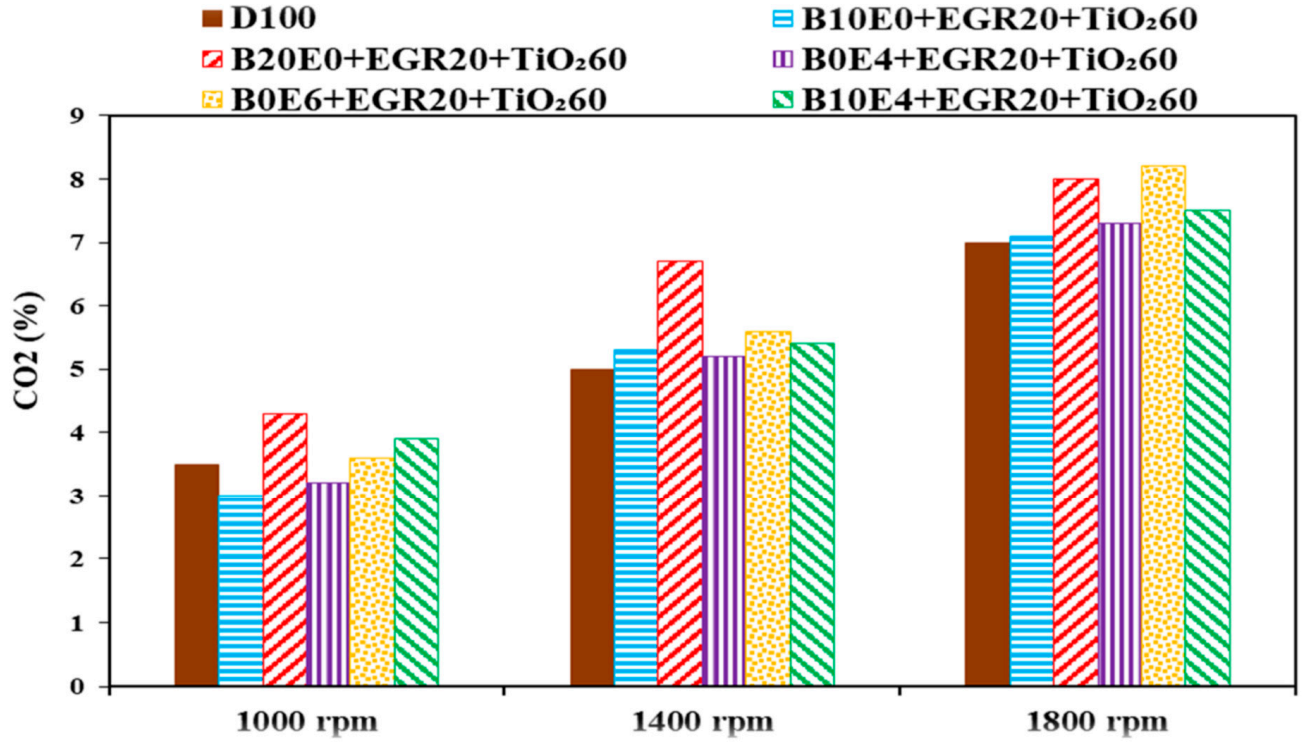

Figure 15. Variation of CO_2 for diesel/ethanol/biodiesel blends at EGR = 20%, TiO_2 = 60 ppm, and various engine speeds.

Figure 15 shows the effect of the simultaneous use of EGR and TiO_2 on CO_2 emission. The maximum amount of CO_2 was observed for B0E6 + EGR20 + $TiO_2$60 by 17.2% at 1800 rpm compared to D100.

3.8. HC Emission

Figure 16 shows the variations of HC emission for the prepared mixtures. As can be seen in all of the prepared mixtures, HC emission is reduced with increasing speed. Incomplete combustion is one of the main reasons for HC formation [42].

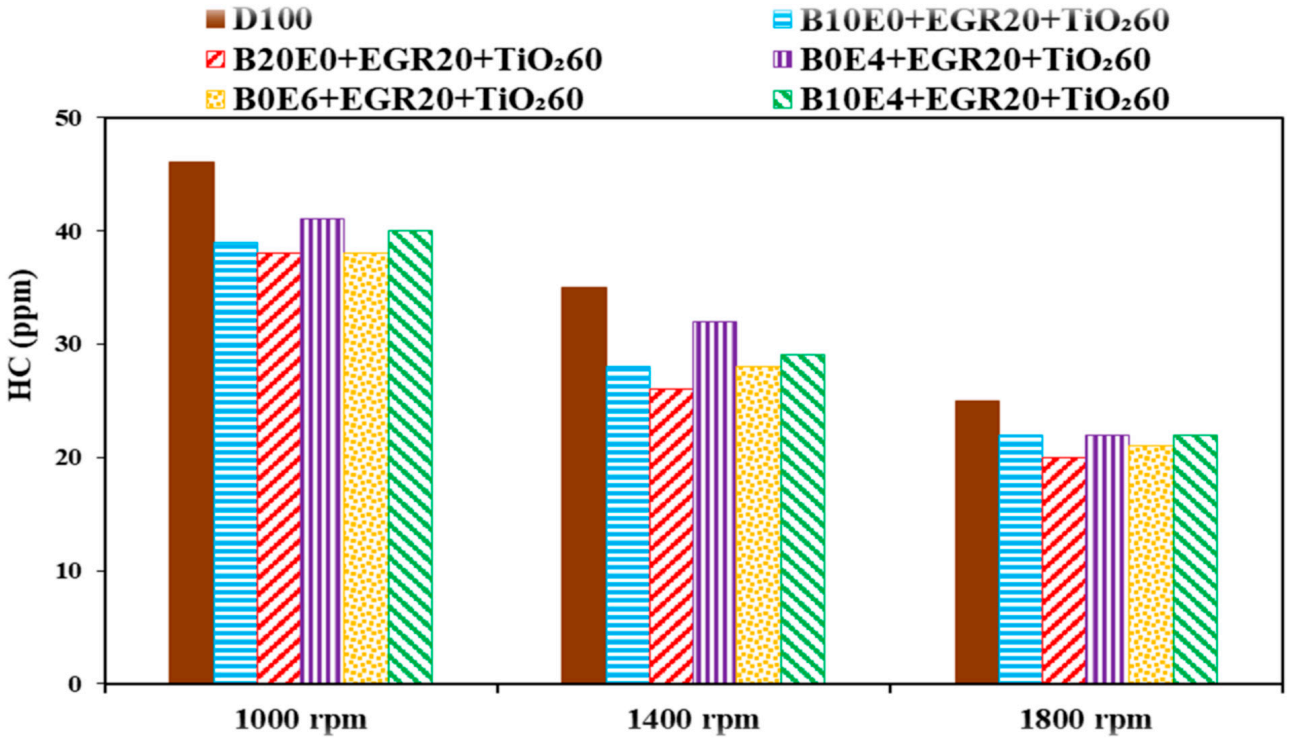

Figure 16. Variation of HC for diesel/ethanol/biodiesel blends at EGR = 20%, TiO_2 = 60 ppm, and various engine speeds.

The higher oxygen content of biodiesel and ethanol than pure diesel, which improves the combustion process, as well as the lower carbon-to-hydrogen ratio of biodiesel and ethanol, can be the main reasons for HC reduction. As can be seen in Figure 16, the minimum HC emission was produced in B20E0 + EGR20 + $TiO_2$60, which reduced HC by 20% at 1800 rpm.

4. Conclusions

In the present study, the performance and emission parameters of a direct injection diesel engine have been experimentally investigated by using different levels of TiO_2 and EGR system in prepared diesel–ethanol–biodiesel blends. The most important results are:

- The minimum power was observed in B20E0 + EGR30, which reduced the power by an average of 27.8% at different speeds.
- With increasing of the EGR rate as well as increasing the percentage of ethanol and biodiesel in the mixture, the brake power and engine torque decreased. While increasing the percentage of TiO_2 in the mixture, the amount of power and torque increased.
- BSFC increased with increasing the EGR rate, as well as increasing the percentage of ethanol and biodiesel in the mixture. However, with increasing the percentage of TiO_2 in the mixture, the amount of BSFC decreased.
- The B10E4 + EGR20 + $TiO_2$60 at 1000, 1400, and 1800 rpm increased BSFC by 4.7, 2.5, and 2% compared to pure diesel.
- Increasing the EGR rate reduced the exhaust gas temperature. While an increase in the percentage of biodiesel, ethanol, and TiO_2 in the mixture increased the exhaust gas temperature.

- The minimum exhaust temperature was recorded for B0E4 + EGR20 + $TiO_2$60, which showed an average reduction of 7% in the exhaust gas temperature compared to D100 at different speeds.
- The amounts of HC and CO emissions increased with increasing of the EGR rate, while the addition of TiO_2, as well as increasing the percentage of biodiesel and ethanol in the mixture, reduced the amounts of these emissions.
- NO_x emissions increased with an increase in the percentage of biodiesel, ethanol, and TiO_2. While increasing the EGR rate reduced NO_x emissions. The minimum amount of NO_x was recorded for B0E4 + EGR20 + $TiO_2$60 with a 13% reduction compared to D100.
- The B10E4 + EGR20 + $TiO_2$60 reduced the emissions of HC, CO, and NO_x by 17, 12.4, and 10% compared to D100. The amounts of brake power and torque were also generated near to pure diesel, while BSFC values increased by an average of 3%.

Author Contributions: Conceptualization, A.Z.A.; methodology, S.P.Y. and A.Z.A.; software, S.P.Y.; validation, R.M., S.P.Y. and A.Z.A.; formal analysis, S.P.Y.; investigation, S.P.Y.; resources, R.M. and A.A.; data curation, S.P.Y.; writing—original draft preparation, S.P.Y.; writing—review and editing, R.M. and A.Z.A.; visualization, S.P.Y.; supervision, R.M., A.A. and A.Z.A.; project administration, A.Z.A.; funding acquisition, A.Z.A. All authors have read and agreed to the published version of the manuscript.

Funding: This research received no external funding.

Data Availability Statement: Data is unavailable due to privacy.

Conflicts of Interest: The authors declare no conflict of interest.

Nomenclature

BSFC = Break Specific Fuel Consumption
CO = Carbon Monoxide
CO_2 = Carbon Dioxide
°C = degrees Celsius
DI = Direct Injection
EGR = Exhaust Gas Recirculation
g/kW-hr = gram per kilowatt hour
g/mol = grams per mole
HC = Hydro Carbon
Kg m^{-3} = Kilogram per cubic meter
kW = Kilo Watt
MJ kg^{-1} = Megajoules per kilogram
mm = millimeter
mm^2 s^{-1} = square millimetre per second
Nm = Newton meter
nm = nanometer
NO_x = Nitrogen Oxides
PM = Particulate Matter
ppm = parts per million
rpm = revolutions per minute
vol% = Volume percent
wt.% = percentage by weight

References

1. Han, J.; Somers, L.; Cracknell, R.; Joedicke, A.; Wardle, R.; Mohan, V.R.R. Experimental investigation of ethanol/diesel dual-fuel combustion in a heavy-duty diesel engine. *Fuel* **2020**, *275*, 117867. [CrossRef]
2. Wu, Y.; Zhang, X.; Zhang, Z.; Wang, X.; Geng, Z.; Jin, C.; Liu, H.; Yao, M. Effects of diesel-ethanol-THF blend fuel on the performance and exhaust emissions on a heavy-duty diesel engine. *Fuel* **2020**, *271*, 117633. [CrossRef]
3. Yesilyurt, M.K. The effects of the fuel injection pressure on the performance and emission characteristics of a diesel engine fuelled with waste cooking oil biodiesel-diesel blends. *Renew. Energy* **2019**, *132*, 649–666. [CrossRef]
4. Rajasekar, E.; Selvi, S. Review of combustion characteristics of CI engines fueled with biodiesel. *Renew. Sustain. Energy Rev.* **2014**, *35*, 390–399. [CrossRef]
5. Suh, H.K.; Lee, C.S. A review on atomization and exhaust emissions of a biodiesel-fueled compression ignition engine. *Renew. Sustain. Energy Rev.* **2016**, *58*, 1601–1620. [CrossRef]
6. Hoekman, S.K.; Broch, A.; Robbins, C.; Ceniceros, E.; Natarajan, M. Review of biodiesel composition, properties, and specifications. *Renew. Sustain. Energy Rev.* **2012**, *16*, 143–169. [CrossRef]
7. Renewable Fuels Association (RFA). *Ethanol Industry Outlook*; Renewable Fuels Association (RFA): St. Louis, MO, USA, 2010; pp. 1–32.
8. Çelebi, Y.; Aydın, H. An overview on the light alcohol fuels in diesel engines. *Fuel* **2019**, *236*, 890–911. [CrossRef]

9. Kim, H.; Choi, B.; Park, S.; Kim, Y. Engine performance and emission characteristics of CRDI diesel engine equipped with WCC and DOC using ethanol blended diesel fuel. In Proceedings of the International Symposium on Alcohol Fuels, San Diego, CA, USA, 26–28 September 2005.
10. Yang, W.M.; An, H.; Chou, S.K.; Chua, K.J.; Mohan, B.; Sivasankaralingam, V.; Raman, V.; Maghbouli, A.; Li, J. Impact of emulsion fuel with nano-organic additives on the performance of diesel engine. *Appl. Energy* **2013**, *112*, 1206–1212. [CrossRef]
11. Nye, M.; Southwell, P. Conversion of rapeseed oil to esters for use as diesel fuel. In Proceedings of the 5th Canadian Bioenergy Research and Development Seminar, Ottawa, ON, Canada, 26–28 March 1984; pp. 487–490.
12. Dorado, M.P.; Ballesteros, E.; Arnal, J.M.; Gomez, J.; Lopez, F.J. Exhaust emissions from a diesel engine fueled with transesterified waste olive oil. *Fuel* **2003**, *82*, 1311–1315. [CrossRef]
13. Karthikeyan, S.; Elango, A.; Prathima, A. Diesel engine performance and emission analysis using canola oil methyl ester with the nano sized zinc oxide particles. *Indian J. Eng. Mater. Sci.* **2014**, *21*, 83–87.
14. Rajesh kumar, B.; Saravanan, S. Effect of exhaust gas recirculation (EGR) on performance and emissions of a constant speed DI diesel engine fueled with pentanol/diesel blends. *Fuel* **2015**, *160*, 217–226. [CrossRef]
15. Yilmaz, N.; Atmanli, A. Experimental assessment of a diesel engine fueled with diesel-biodiesel-1-pentanol blends. *Fuel* **2017**, *191*, 190–197. [CrossRef]
16. Devarajan, Y.; Munuswamy, D.B.; Mahalingam, A. Investigation on behavior of diesel engine performance, emission, and combustion characteristics using nano-additive in neat biodiesel. *Heat Mass. Transf.* **2019**, *55*, 1641–1650. [CrossRef]
17. Uyumaz, A. Experimental evaluation of linseed oil biodiesel/diesel fuel blends on combustion, performance and emission characteristics in a DI diesel engine. *Fuel* **2020**, *267*, 117150. [CrossRef]
18. Uyumaz, A. Combustion, performance and emission characteristics of a DI diesel engine fueled with mustard oil biodiesel fuel blends at different engine loads. *Fuel* **2018**, *212*, 256–267. [CrossRef]
19. Kim, H.Y.; Ge, J.C.; Choi, N.J. Effects of ethanol–diesel on the combustion and emissions from a diesel engine at a low idle speed. *Appl. Sci.* **2020**, *10*, 4153. [CrossRef]
20. Wu, Q.; Xie, X.; Wang, Y.; Roskilly, T. Effect of carbon coated aluminum nanoparticles as additive to biodiesel-diesel blends on performance and emission characteristics of diesel engine. *Appl. Energy* **2018**, *221*, 597–604. [CrossRef]
21. Ahmed, A.; Shah, A.N.; Azam, A.; Uddin, G.M.; Ali, M.S.; Hassan, S.; Ahmed, H.; Aslam, T. Environment-friendly novel fuel additives: Investigation of the effects of graphite nanoparticles on performance and regulated gaseous emissions of CI engine. *Energy Convers. Manag.* **2020**, *211*, 112748. [CrossRef]
22. Aldhaidhawi, M.; Chiriac, R.; Bădescu, V.; Descombes, G.; Podevin, P. Investigation on the mixture formation, combustion characteristics and performance of a Diesel engine fueled with Diesel, Biodiesel B20 and hydrogen addition. *Int. J. Hydrogen Energy* **2017**, *42*, 16793–16807. [CrossRef]
23. Arul Mozhi Selvan, V.; Anand, R.B.; Udayakumar, M. Effect of cerium oxide nanoparticles and carbon nanotubes as fuel-borne additives in diesterol blends on the performance, combustion and emission characteristics of a variable compression ratio engine. *Fuel* **2014**, *130*, 160–167. [CrossRef]
24. Wu, H.W.; Hsu, T.T.; Fan, C.M.; He, P.H. Reduction of smoke, PM 2.5, and NO_x of a diesel engine integrated with methanol steam reformer recovering waste heat and cooled EGR. *Energy Convers. Manag.* **2018**, *172*, 567–578. [CrossRef]
25. Pan, M.; Zheng, Z.; Huang, R.; Zhou, X.; Huang, H.; Pan, J.; Chen, Z. Reduction in PM and NO_x of a diesel engine integrated with n-octanol fuel addition and exhaust gas recirculation. *Energy* **2019**, *187*, 115946. [CrossRef]
26. Lapuerta, M.; Armas, O.; Garcia-Contreras, R.G. Stability of diesel–bioethanol blends for use in diesel engines. *Fuel* **2007**, *86*, 1351–1357. [CrossRef]
27. Hansen, A.C.; Zhang, Q.; Lyne, P.W.L. Ethanol–diesel fuel blends—-A review. *Bioresour. Technol.* **2005**, *96*, 277–285. [CrossRef] [PubMed]
28. Arcoumanis, C.; Bae, C.; Crookes, R.; Kinoshita, E. The potential of di-methyl ether (DME) as an alternative fuel for compression-ignition engines: A review. *Fuel* **2008**, *87*, 1014–1030. [CrossRef]
29. Baert, R.S.; Beckman, D.E.; Veen, A. *Efficient EGR Technology for Future HD Diesel Engine Emission Targets*; SAE Technical Paper 1999-01-0837; SAE International: Warrendale, PA, USA, 1999. [CrossRef]
30. Mobasheri, R.; Khabbaz, S. *Modeling the Effects of High EGR Rates in Conjunction with Optimum Multiple Injection Techniques in a Heavy Duty DI Diesel Engine*; SAE Technical Paper 2014-01-1124; SAE International: Warrendale, PA, USA, 2014. [CrossRef]
31. Kökkülünk, G.; Parlak, A.; Ayhan, V.; Cesur, I.; Gonca, G.; Boru, B. Theoretical and experimental investigation of steam injected diesel engine with EGR. *Energy* **2014**, *74*, 331–339. [CrossRef]
32. Pirouzpanah, V.; Khoshbakhti Sarai, R. Reduction of emissions in an automotive direct injection diesel engine dual-fuelled with natural gas by using variable exhaust gas recirculation. *Proc. Inst. Mech. Eng.* **2003**, *217*, 719–725. [CrossRef]
33. Örs, I.; Sarıkoç, S.; Atabani, A.E.; Ünalan, S.; Akansu, S.O. The effects on performance, combustion and emission characteristics of DICI engine fuelled with TiO_2 nanoparticles addition in diesel/biodiesel/n-butanol blends. *Fuel* **2018**, *234*, 177–188. [CrossRef]
34. Saxena, V.; Kumar, N.; Kumar Saxena, V. A comprehensive review on combustion and stability aspects of metal nanoparticles and its additive effect on diesel and biodiesel fuelled CI engine. *Renew. Sustain. Energy Rev.* **2017**, *70*, 563–588. [CrossRef]
35. D'Silva, R.; Binu, K.; Bhat, T. Performance and emission characteristics of a CI engine fuelled with diesel and TiO_2 nanoparticles as fuel additive. *Mater. Today Proc.* **2015**, *2*, 3728–3735. [CrossRef]

36. Fangsuwannarak, K.; Triratanasirichai, K. Effect of metalloid compound and bio-solution additives on biodiesel engine performance and exhaust emissions. *Am. J. Appl. Sci.* **2013**, *10*, 1201–1213. [CrossRef]
37. SinghYadav, V.; Soni, S.L.; Sharma, D. Performance and emission studies of direct injection CI engine in duel fuel mode (hydrogen-diesel) with EGR. *Int. J. Hydrogen Energy* **2012**, *37*, 3807–3817. [CrossRef]
38. Selvan, T.; Nagarajan, G. Combustion and emission characteristics of a diesel engine fuelled with biodiesel having varying saturated fatty acid composition. *Int. J. Green Energy* **2013**, *10*, 952–965. [CrossRef]
39. Egnell, R. *The Influence of EGR on Heat Release Rate and NO Formation in a DI Diesel Engine*; SAE Technical Paper 2000-01-1807; SAE International: Warrendale, PA, USA, 2000. [CrossRef]
40. Agarwal, D.; Kumar Singh, S.; Kumar Agarwal, A. Effect of exhaust gas recirculation (EGR) on performance, emissions, deposits and durability of a constant speed compression ignition engine. *Appl. Energy* **2011**, *88*, 2900–2907. [CrossRef]
41. Sadhik Basha, J.; Anand, R. An experimental study in a CI engine using nanoadditive blended water–diesel emulsion fuel. *Int. J. Green Energy* **2011**, *8*, 3332–3348.
42. Wang, W.G.; Lyons, D.W.; Clark, N.N.; Gautam, M.; Norton, P.M. Emissions from nine heavy trucks fueled by diesel and biodiesel blend without engine modification. *Environ. Sci. Technol.* **2000**, *34*, 933–939. [CrossRef]